Inverse Analysis of Deep Excavation using Differential Evolution Algorithm

B. D. Zhao[1], L. L. Zhang[2]*, D. S. Jeng[3], J. H. Wang[4], J. J. Chen[5]

[1] Graduate research student, Department of Civil and Architectural Engineering, City University of Hong Kong, Hong Kong. E-mail: bdzhao2-c@my.cityu.edu.hk. Previous graduate student, Civil Engineering Department, Shanghai Jiaotong University, Shanghai, China.

[2]*Corresponding author, Associate Professor, Center for Marine Geotechnical Engineering, State Key Laboratory of Ocean Engineering, Civil Engineering Department, Shanghai Jiaotong University, Shanghai, 200240, China. E-mail: lulu_zhang@sjtu.edu.cn

[3]Professor, Griffith School of Engineering, Griffith University Gold Coast Campus, Queensland QLD 4222, Australia and Zhi-Yuan Chair Professor, Center for Marine Geotechnical Engineering, State Key Laboratory of Ocean Engineering, Shanghai Jiaotong University, Shanghai 200240, China. E-mail: jengd2@asme.org

[4]Professor, Center for Marine Geotechnical Engineering, State Key Laboratory of Ocean Engineering, Shanghai Jiaotong University, Shanghai 200240, China. E-mail: wjh417@sjtu.edu.cn

[5]Associate Professor, Center for Marine Geotechnical Engineering, State Key Laboratory of Ocean Engineering, Civil Engineering Department, Shanghai Jiaotong University, Shanghai, 200240, China. E-mail: chenjj29@sjtu.edu.cn

Revision submitted to: **International Journal for Numerical and Analytical Methods in Geomechanics**

November 2013

7000 words, 14 figures, 4 tables

ABSTRACT

This paper presents the applications of the Differential Evolution (DE) algorithm in back analysis of soil parameters for deep excavation problems. A computer code, named Python-based Differential Evolution (PyDE), is developed and incorporated into the commercial finite element software ABAQUS, with a parallel computing technique to run FE analysis for all trail vectors of one generation in DE in multiple cores of a cluster, which dramatically reduces the computational time. A synthetic case and a well instrumented real case, i.e., the Taipei National Enterprise Center (TNEC) project, are used to demonstrate the capability of the proposed back-analysis procedure. Results show that multiple soil parameters are well identified by back-analysis using DE optimization algorithm for highly nonlinear problems. For the synthetic excavation case, the back-analyzed parameters are basically identical to the input parameters which are used to generate synthetic response of wall deflection. For the TNEC case with totally nine parameters to be back-analyzed, the relative errors of wall deflection for the last three stages are 2.2%, 1.1% and 1.0%, respectively. Robustness of the back-estimated parameters is further illustrated by a forward prediction. The wall deflection in the subsequent stages can be satisfactorily predicted using the back analyzed soil parameters at early stages.

Keywords: Excavations, Inverse analysis, Differential Evolution, Optimization Algorithms, Deflection, Cam-clay model

INTRODUCTION

In urban area, the construction safety of a deep excavation becomes crucial with the increase of building density. It is critical important to predict and control the ground movement and structure deformation of a deep excavation during the construction procedure. Numerical modeling which is commonly used in the design and construction process [1-3], can provide a better understanding of soil behavior during the construction, verify performance of a highly complex excavation through comparison with field observations and further predict future performance [4-6]. However, accurate prediction of deformations due to deep excavation using numerical tools is still complicated for engineers. The accuracy of numerical simulation of deep excavation depends greatly on the selection of constitutive models and determination of appropriate soil parameters [7]. Although comprehensive laboratory and in situ tests can be conducted, there are some difficulties in the precise determination of the soils parameters due to sample disturbance and measurement error [8]. Furthermore, even with well measured soil parameters from laboratory or in situ tests, the estimated performance still deviate from the field observation due to inherent spatial variability [9, 10] and inadequacy of the simulation model itself [11].

Detailed observations can provide better understanding of the behavior of a deep excavation and make the design and construction procedure more rational [12-14]. To determine the representative soil parameters based on field observations, back analysis or inverse analysis approaches have been adopted in both deterministic and probabilistic approaches [15-21]. The back analysis methods are basically based on different kinds of optimization techniques, which allows the performance of inverse analyses in a more rational and objective manner. The optimization methods for back analysis can be divided into three groups based on algorithms, i.e., direct methods, gradient based methods [17, 22] and artificial intelligence algorithm based methods [23-24]. Direct methods only need evaluations of the function and do not require gradient calculations of the error function, and therefore are easy to implement. Some

commonly-used direct optimization methods are the Univariate method, Pattern Search, the Powell method and the ordinary Simplex method. Gradient-based methods, such as the Steepest Descent, the Conjugate Gradient, the Newton methods, can accelerate the optimization progress but need to evaluate derivatives. It has been reported in the literature that direct and gradient based methods are not sufficient for high dimensional, strongly non-convex or flat error function, conditions with multiple correlated parameters. Among these, Finno and Calvello [17] conducted model calibration for the parameters in the Hardening-Soil (H-S) model using a modified Gauss–Newton method. Tang and Kung [22] applied the quasi-Newton method for back analysis of excavation-induced wall deflection. Zentar et al. [25] combined the steepest decent method with the Levenberg–Marquardt method and identified the Modified Cam-Clay (MCC) parameters based on the pressuremeter test data. They all found that simultaneously back analysis highly correlated parameters may not yield a unique optimized solution. In addition, optimization results by the gradient based method may depend on the choice of initial parameter values [17].

The artificial intelligence algorithm based methods, including neural network method, annealing method, swarm intelligence algorithms, evolution strategies, genetic algorithms, etc., are known to be robust and efficient to solve very complex problems and are considered as global optimization methods compared with the local optimization methods such as gradient based methods [26-29]. The applications of artificial intelligence based methods, especially the Darwin's theory of evolution inspired algorithms such the genetic algorithms and the evolution algorithms, in geotechnical problems, have been increased in recent years. These evolution-inspired algorithms are stochastic global search techniques and are recognized to be highly efficient in dealing with large, discrete, non-linear and poorly understood optimization problems. As the most popular evolution-inspired algorithm applied in geomechnics, the GA algorithm has been employed to solve various problems such as characterization of discontinuity in fractured rocks [30-32], parameter identification

of constitutive models [24, 32, 33], identification of critical slip surfaces in slope stability analysis [34-35], optimization of pile group design [36], and reliability analysis [37]. When applied in the back analysis of excavation problems, the GA algorithm is found to be able to identify the best solution of the problem even with a flat or noisy error function [24, 30, 38].

There are several drawbacks of the classic GA algorithm by Holland (1982) [39]. First, the parameters are represented by binary strings and the binary strings are decoding into real numbers by interpolation within the ranges of each parameter. This choice limits the resolution with which an optimum can be located to the precision set by the number of bits in the integer. Second, only a portion of parents which have relatively high fitness is selected for reproduction. The selected parents are mixed with their generated children as a secondary generation and use random mutation for diversity. However, there is no guarantee that the best-so-far solution will not be lost, although cross-over and random mutation schemes are used [40].

The Differential Evolution (DE) algorithm [41-43], which is similar to GA, emerged as a very competitive form of evolutionary computing in the late 90's. The DE algorithm was sometimes considered as a variant of GA in literature because they are identical with respect to their major optimization process such as selection, mutation and recombination/crossover. However, it exhibit significant differences with respect to the selection scheme, the encoding of the variables and especially the self-adaptation of the parameters. Hence, DE and GA are considered as different classes of evolution computing algorithms [44].

The major difference between DE and GA is the difference vector based mutation, which is also the core idea and main strength of DE. DE generates new parameter vectors by adding the scaled difference vector between two population members to a third member (the base vector). While in GAs, mutation is treated as a random change of some parameter. The advantage of the difference vector based mutation is that both the step size and the orientation of a mutation can be automatically adapted to the

objective function landscape and hence it promotes basin-to-basin transfer, where search points may move from one local minimum to another one [42, 44].

Secondly, most GAs use crossing two vectors to produce two trial vectors, often by one-point crossover, which means randomly selecting a single crossover point such that all parameters to the left of the crossover point are inherited from vector 1, while those to the right are copied from the vector 2 and constructing a second trial vector by reversing the roles of the two vectors. However, DE uses a binary n-point crossover to generate one trial vector. Thirdly, DE and GA are different in selection scheme. In parent selection scheme, unlike GAs that select parents based on their fitness, DE gives all the individuals equal chance for being selected as parents and the base vectors are randomly picked up without any regard for their fitness values. In survivor selection scheme, DE employs a one to one competition where each parent vector competes once only against its own offspring. Parent-offspring competition has a superior ability to maintain population diversity when compared with ranking or tournament selection where elites and their offspring may dominate the population rapidly. DE algorithm also has flexibility to handle different kind of constraints on the unknown parameters with a robust convergence [44]. In addition, DE uses floating-point numbers that are more appropriate than decoded binary strings for representing points in continuous space and uses computer resources efficiently. Certainly, some real-coded GAs have also been developed to handle this problem.

Amorim et al. (2012) [45] compared the performance of GA and DE for solving a history mapping inverse problem in oil reservoir engineering. GA performed better than DE on the initial generations, i.e., the objective error function value dropped much faster in the beginning of GA than DE. However, once close to the region of a good solution, GA was not successful in refining this possible solution. On the other hand, DE could refine very well the solutions and achieved impressive fitness values. For the problems with different numbers of target parameters from 2 to 16, DE could all produce smaller relative errors between the target parameter vector and the

optimized parameters obtained. When the number of parameters is greater five, the relative error between the target parameter vector and the optimized parameters obtained by DE is around 10% of that of GA.

The application of DE in geotechnical engineering emerges in recent years. Vardakos et al. (2012) [46] conducted a back analysis of tunneling using the Differential Evolution and showed that DE exhibits excellent convergence, repeatability characteristics. Xing et al. (2013) [47] combined the support vector machine method and DE algorithm for optimization of tunnel construction process.

Although comprehensive investigations have been conducted using the classic GA algorithm in back analysis of excavation problems, the ability of DE in back analyzing braced excavation problems has not been examined based on the authors' knowledge. The application of evolutionary computing algorithms in excavation back analysis should be further explored. In the previous back analyses of excavation using GA or other artificial intelligence algorithm based methods, the scale of the problem (in terms of number of optimization parameters) is often limited to less than five parameters and relatively simple constitutive soil models. As the scale and the characteristic of the problem may greatly influence the shape of objective function and hence the performance of the optimization method [44, 45], real case studies with more soil layers and more parameters to identify and complex constitutive law should be conducted to reinforce the applicability of evolutionary based algorithms.

In this paper, we investigate the potential use of the Differential Evolution in the back-analysis of braced excavation response. A computer code named Python-based Differential Evolution (PyDE) is developed using the objective-oriented language Python and implemented in the commercial FEM software ABAQUS. As the high computational cost is a common drawback of evolutionary based algorithms [42, 44], a parallel computing technique is used to run parallel FE analysis for one generation in multiple cores of a computer cluster and dramatically reduce the computational time. The implementation of the back analysis method based on DE and its

computational performance are demonstrated using both a synthetic excavation problem and a complex real case, i.e., the Taipei National Enterprise Center (TNEC) project, in which nine parameters of Modified Cam-clay (MCC) are estimated. The efficiency and convergence characteristics using DE are discussed. Furthermore, the robustness of the back-estimated parameters is illustrated by a forward prediction, where field observations during early stages of excavation to predict wall deflections during later stages.

METHODOLOGY OF BACK ANALYSIS FOR EXCAVATION

Objective Function of Back Analysis

The match of simulated results to the observations is one of the most important indicators of how well a model represents an actual system. The difference between the simulated result and observed result is measured by an objective function. To determine the optimized soil parameters by back analysis, the soil parameters are updated repeatedly through iteration process until the simulated result is close enough to the observed result. Some commonly-used objective functions are least-squares/weighted least-squares objective function [23, 24], maximum likelihood [15], and Bayesian posterior probability [18-21]. In this study, a normalized form of least-square objective function is adopted [22]:

$$f(\mathbf{X}) = \frac{1}{N}\sum_{i=1}^{N}\left(\frac{d_i(\mathbf{X})}{d_i^*} - 1\right)^2 \tag{1}$$

where N is the number of measurement points that used to back-figure the target parameters in the optimization procedure, d_i^* is the observed result and $d_i(\mathbf{X})$ is the simulated result, $\mathbf{X} = [x_1, x_2 ... x_m]^T$ is the vector of m input parameters. In particular, for wall deflection of a braced excavation, N is the number of measurement points for a vertical cross section of the wall; d_i^* is the measured wall deflection at point i; d_i is

the calculated wall deflection at point *i* based on numerical modeling. The advantage of the normalized least-square or relative error objective function is that different types of measurements such as surface settlement, bracing load and pore water pressure response could be incorporated to extract the soil parameters. However, the normalized objective function may be give preference to small values of experimental data and is not defined by observed zero values. In addition, the uncertainty in the field measurements is not considered. Some researchers used the scalar or weighted least square function with the weights related with the uncertainty of measurement. The uncertainty based weights however are selected based on engineering judgment [24, 29]. For the least-square objective function, it is hard to know the appropriate number of measured data to use specifically when different measurement types are to be combined and the interval between measurement points may affect the objective function. To make the objective function independent of the interval between the measurement points, the area between the experimental and the computational curves could be used as the objective function [33]. Effect of different types of objective functions is out of the scope of this study and will be further investigated in another paper.

Optimization using Differential Evolution

Evolutionary algorithms are stochastic optimization methods inspired on Darwin's evolution theory and natural selection [44]. There are many different variants of evolutionary algorithms and the common underlying idea behind all these techniques is the same: given a population of individuals, recombination and/or mutation, and natural selection (survival of the fittest), which causes a rise in the fitness of the population. Storn and Price [41-42] proposed an evolutionary algorithm called the Differential Evolution (DE). DE uses floating-point instead of bit-string encoding and

arithmetic operations instead of logical ones. No special routine is needed to define, input, manipulate or output the floating-point format because the most common programming languages support this format. In binary system, a parameter was changed by inverting or "flipping" a bit. For example, if the initial parameter value is 15 (01111 binary) and the optimal value is 16 (10000 binary), the probability of this improving move happen is p_5, where p is the probability of a bit was inverted. Generally speaking, floating-point numbers and manipulating them with arithmetic operators offer advantages over the classic GA "bit flipping" approach including (a) easy to use, (b) efficient memory utilization, (c) lower computational complexity, (d) lower computational effort – fast convergence and (e) greater freedom in designing a mutation distribution [42].

A typical DE algorithm includes processes of initialization, mutation, crossover and selection. Details of the four processes are as follows:

(1) Initialization

Assume there are N_p vectors of input parameter in each generation as shown in Fig. 1. The i_{th} parameter vector in g_{th} generation is $\mathbf{X}_{i,g}$ as an individual that could produce a unique objective function value. The j_{th} parameter value of $\mathbf{X}_{i,g} = [x_{0,i,g}, x_{1,i,g} \cdots, x_{D-1,i,g}]$ is denoted as $x_{j,i,g}$. D is the dimension of the parameter vector. Before the population is initialized, the upper and lower bounds for each parameter should be specified based on experience or tests. The j_{th} parameter value of i_{th} parameter vector in the first population, $x_{j,i,0}$, can be determined by a random number generator once the bounds are specified.

$$x_{j,i,0} = rand(0,1) \times (b_{j,U} - b_{j,L}) + b_{j,L} \quad (2)$$

where $rand(0,1)$ is a random number from an uniform distribution $U(0,1)$, $b_{j,U}$ and $b_{j,L}$ are the upper bound and the lower bound of the j_{th} parameter, respectively.

Babu and Sastry [40] , Vardakos et al. [46] and Chakraborty [43] showed that DE algorithm can converge to the global optimum irrespective of the initial random generated population.

(2) Difference vector based mutation

Select $\mathbf{X}_{i,g}$ as a trial vector for genetic operation. Three other vectors, $\mathbf{X}_{r0,g}$, $\mathbf{X}_{r1,g}$ and $\mathbf{X}_{r2,g}$, are randomly selected from the remaining vectors from the g_{th} generation. A mutant vector $\mathbf{V}_{i,g} = [v_{0,i,g}, v_{1,i,g} \cdots, v_{D-1,i,g}]$ is generated as:

$$\mathbf{V}_{i,g} = \mathbf{X}_{r0,g} + F \times (\mathbf{X}_{r1,g} - \mathbf{X}_{r2,g}) \quad (3)$$

where F is the constant mutation scaling factor. According to Storn and Price [34], the optimum value of F can be taken from 0.4 to 1.0. F only affects the relative step size since the distribution of difference vectors is itself adaptive. For example, we have 5 vectors in one generation (Figure 2a). The number of all possible non-zero difference vectors (pair to pair) is 4×5. Figure 2(b) illustrates 20 non-zero difference vectors generated by the five vectors in Figure 2(a). In the graph, differentials have been scaled by half (F = 0.5), and transported to a common origin. Note that the distribution is symmetric about zero because every pair of vectors gives rise to two opposite but equal difference vectors. Thus, F can be kept constant during optimization without compromising DE's ability to generate steps of the required size [42-43]. With a scaling factor F and the difference vector together, it can ensures that the mutation vectors do not duplicate existing points. In addition, scaling can shift the focus of the search between local and global if the scaling factor is reasonable [42].

Difference vector based mutation is the major difference between DE and GA. In classic GA, some of the individuals are randomly mutated by inversion of one byte on

individual chain. The advantage of the difference vector based mutation is that both the step size and the orientation of a mutation can be automatically adapted to the objective function landscape and hence promising regions of the fitness landscape are investigated automatically once they are detected and it promotes basin-to-basin transfer, where search points may move from one local minimum to another one [42, 44].

(3) Crossover

In order to increase the diversity of the perturbed parameter vectors, crossover is introduced. A new trial vector $\mathbf{U}_{i,g} = [u_{0,i,g}, u_{1,i,g} \cdots, u_{D-1,i,g}]$ is created from the original trial vector $\mathbf{X}_{i,g}$ and the mutant vector $\mathbf{V}_{i,g}$:

$$u_{j,i,g} = \begin{cases} v_{j,i,g} & \text{if } (rand(0,1) \le Cr \text{ or } j = j_{rand}) \\ x_{j,i,g} & \text{otherwise.} \end{cases} \quad (4)$$

where $Cr \in [0,1]$ is a crossover constant and j_{rand} is a random chosen index $\in [0,1,2,...,D]$. The crossover probability, *Cr*, is a user-defined value that controls the fraction of parameter values that are copied from the mutant. To determine which source contributes a given parameter, the crossover compares *Cr* to the output of a uniform random number generator, rand(0,1). If the random number is less than or equal to *Cr*, the trial parameter is inherited from the mutant, $\mathbf{V}_{i,g}$; otherwise, the parameter is copied from the original trial vector vector, $\mathbf{X}_{i,g}$. It means that the j_{rand} th parameter will inherent from the mutant vector and each of the other (*D*-1) parameters will have *C*r probability to inherent from the mutant vector. Figure 3 illustrates the process of binary n-point crossover in DE.

In boundary-constrained problems, it is essential to ensure that the reproduced parameter values lie inside their allowed ranges otherwise the results could be unreasonable and the problem may not converge. In this study, parameter values in the new trial vector that violate boundary constraints are replaced with random numbers

generated within the feasible range [48]:

$$u_{j,i,g} = \begin{cases} rand(0,1) \times (b_{j,U} - b_{j,L}) + b_{j,L} & if \quad u_{j,i,g} \notin [b_{j,L}, b_{j,U}] \\ u_{j,i,g} & otherwise \end{cases} \tag{5}$$

(4) Selection. By comparing the objective function values of $\mathbf{U}_{i,g}$ with $\mathbf{X}_{i,g}$, the individual with the lower objective function value is selected to next generation.

$$\mathbf{X}_{i,g+1} = \begin{cases} \mathbf{U}_{i,g} & if \quad f(\mathbf{U}_{i,g}) \le f(\mathbf{X}_{i,g}) \\ \mathbf{X}_{i,g} & otherwise \end{cases} \tag{6}$$

The same procedure is followed for all N_P parameter vectors in each generation and new N_P parameter vectors are formed for the next generation. The above evolution of generation is repeated until a maximum of generation is reached or the minimum objective function for one generation is less than a given error. The parameter vector of the last generation is then considered as the optimal or back estimated parameter vector.

Development of PyDE Code in ABAQUS

In this study, a computer code named Python-based Differential Evolution (PyDE) is developed using an open-source objective-oriented language Python to implement back analysis with the DE algorithm in the well-known commercial FEM package ABAQUS. Python language is a high-level programming language that supports object-oriented programming and allows easy integration with software programmed in Fortran, C, C++, and other languages. It provides a clear and readable syntax and is highly stable and can be easily transformed to different operating systems. It also includes a large set of standard libraries and its open-source license enables the modification and distribution of Python-based applications with almost no restrictions. Moreover, as the standard programming language of ABAQUS, Python can easily change the model data, such as material parameters and structure geometry, and read the resulting output databases. The interaction between PyDE code and ABAQUS in the back analysis is shown in the flowchart in Fig. 4. In the PyDE code, the trial vector,

345 $\mathbf{X}_{i,g}$, is selected and the new trial vector $\mathbf{U}_{i,g}$ is developed through mutation and
346 crossover. After that, the two parameter vectors are imported into ABAQUS as input
347 parameters for the FEM analysis. The results of numerical analysis are used to
348 calculate the objective function and the selection of trail vector for the next generation
349 is made. If the objective function is less than a given value or the maximum number of
350 generations is reached, the inverse analysis procedure is terminated.
351 As the high computational cost is a common drawback of evolutionary based
352 algorithms, a parallel computing technique is used to run parallel FE analysis for each
353 parameter vector of one generation in multiple cores of a computer cluster and this
354 can dramatically reduce the computational time. Assume one generation with 90
355 individual parameter vectors. If each FEM calculation takes 1 minute of CPU time,
356 then 9000 minutes (about 6 days) are needed for 100 generations. In this study, the 90
357 FEM simulations in one generation were submitted at the same time to 90 CPUs of
358 the computer cluster. Therefore, the back analysis can be finished in several hours.
359

360 ## EXAMPLE APPLICATION: SYNTHETIC EXCAVATION CASE

361 For a complex excavation site, there are usually multiple soil layers and a number of
362 soil parameters should be considered in simulation of the excavation. Multiple soil
363 parameters may greatly increase the difficulty of back analysis and affect its efficacy.
364 On the other hand, a synthetic case instead of real complex excavation problems can
365 reduce the difficulty of back analysis for a highly nonlinear problem and avoid the
366 unknown errors from the measurement data [24]. Hence, to examine the efficacy and
367 robustness of the back analysis approach for excavation problems, we start with a
368 synthetic excavation case with only one soil layer.

369 **Numerical Model of the Synthetic Case**

370 The synthetic case is a 6 m deep and 20 m wide excavation zone with only one layer
371 of clayey soil, as shown in Fig. 5. The retaining wall is 0.6 m thick and 12 m deep.

The excavation is conducted in one step and a strut is installed at the level of ground surface to support the retaining wall. In the finite element simulation, due to the geometric symmetry, only a half of the excavation is modeled under plain strain condition. The overall model size is 50 m long and 25 m high, which is considered large enough to avoid boundary constraints. The left boundary is x-symmetric, which means the vertical displacement is allowed however the horizontal direction displacement and rotation is fixed. The boundary on the right side is also fixed along horizontal direction and the vertical direction is free. The bottom boundary is fixed along both horizontal and vertical directions. The Modified Cam-clay (MCC) constitutive model is adopted for the clayey soil in this excavation site. The retaining structure including the retaining wall and the strut are assumed to be linear-elastic. The element type for the soil is 4-node bilinear rectangular element. Spring element and 2-node linear beam element are adopted for the strut and the retaining wall, respectively.

Sensitivity Study of Soil Parameters

Prior to the back analysis, a sensitivity study is conducted to find out the most important soil parameters which can affect the wall deflection of the excavation. Four soil parameters of the MCC model, including the slope of the critical state line in the q-p' plane (M), the slope of isotropic normal consolidation line in the e-ln(p') diagram (λ), the slope of isotropic swelling/recompression line in the e-ln(p') diagram (κ), and the Poisson's ratio (ν), are selected for sensitivity analysis. In addition, as the soil-wall interface may also affect wall deflection [49], the friction coefficient μ for the interface between the wall and surrounding soil is also chosen for the sensitivity analysis. In the benchmark case, the values of ν, κ, λ, M and μ are 0.2, 0.014, 0.14, 1.2 and 0.2, respectively. Then, each parameter is varied according to the values listed in Table 1, while the other four parameters keep the values in the benchmark case. All values vary within the representative ranges for clayey soils [50, 51]. The soil unit

399 weight γ of the clay soil layer is 18.0 kN/m3. The void ratio e and the coefficient of
400 earth pressure at rest K_0 are assumed to be 1.0 and 1.0, respectively. The Young's
401 modulus and the Poisson's ratio of the retaining wall are assumed to be 12 GPa and
402 0.2, respectively. The stiffness of the strut is assumed to be 10,000 KN/m. Numerical
403 simulations with these values of input parameters can produce a reasonable shape of
404 wall deflection according to the previous studies of numerical simulations and field
405 measurement [52].
406 Fig. 6 shows the sensitivity of the wall deflection on the five parameters. It can be
407 seen that the variation of λ and μ have little effect on the wall deflection. However,
408 the variation of ν, κ and M have significant effects on the deformation of the wall.
409 During the excavation, the soil in front of the wall is in the unloading condition which
410 is directly related to the swelling index κ [11]. The Poisson's ratio ν has a significant
411 effect on the wall deflection because it affects the shear modulus (G) of the soil. The
412 slope of the critical state line in the q-p' plane (M) has the most significant effects
413 especially when it has a small value 0.8 since it affects the plastic surface shape and
414 the soil can enter the plastic zone easily with a small value of M. It is also considered
415 as an important parameter to be indentified in back analysis of pressuremeter test data
416 [25] or traxial test data [51]. A quantitative sensitivity analysis is conducted for the
417 five parameters in terms of the variation of objective function with respect to the
418 variation of each parameter. The horizontal wall deflection simulated using the
419 parameters of the benchmark case in the sensitivity study were used as the synthetic
420 observation data. The relative error objective function is calculated based on the
421 results in Figure 6. The dimensionless sensitivity coefficients $S_i = \frac{\Delta f / \Delta x_i}{f / x_i}$ [53], of ν,
422 κ, λ, M and μ with respect to the benchmark case are 3.45, 0.97, 0.57, 1.02, 0.56,
423 respectively. Therefore, in this paper, the three parameters, ν, κ and M, are selected as
424 the target parameters to be identified in the back analysis of excavation. It should be
425 noted that different kinds of quantitative parameter sensitivity analysis could be used

to further describe the effects of these parameters on the wall deflection. However, due to the limited length of this paper they are not implemented in this paper and the back analyzed results shows that using these three parameters are enough to reach satisfactory wall deflections.

Back Analysis of Soil Parameters Using Synthetic Data

The horizontal wall deflection simulated using the parameters of the benchmark case in the sensitivity study were used as the synthetic observation data. The upper and lower bounds of the three target soil parameters in the back analysis are listed in Table 2. According to [41-42], three DE's control variables, namely population size N_p, mutation scaling factor F and crossover probability Cr, are set as 30 ($10\times m$), 0.5 and 0.9, respectively. The target value for the objective function is 0.01% and the maximum generation number is 50. The back analysis is terminated at the 47_{th} generation with the minimum objective function value of 4.4×10^{-5}. As shown in Table 2, the optimized parameters are basically the same as the input parameters, which illustrates that the exact values of the three parameters of the MCC model can be accurately back-analyzed.

Fig. 7 shows the contour of the objective function and the iteration path of the two parameters (ν and M). The contour of the objective function is constructed using all calculation results of the 47 generations. Although, the objective function value is actually determined by the three parameters used in back analysis, this graph clearly shows the convergence of objective function. If the objective functions on other space (M and κ) or (ν and κ) illustrate the similar contours and iteration paths. Fig. 8 presents the evolution process of the objective function value and the soil parameters using the boxplots of the objective functions and back estimated parameters in 1_{st}, 10_{th}, 20_{th}, 30_{th}, 40_{th} and 47_{th} generations. The top and bottom of the box represent the 25th and 75th percentiles of the back-estimated parameter. A horizontal line near the middle of the box identifies the median value. The minimum and maximum values of the parameter are also shown in the boxplot. As can be seen, the objective function

value experienced a significant decrease during the first ten generations and are reducing at a lower speed for the following generations. The soil parameters in the first generation are widely distributed, while in the 47th generation the distributions of the parameters are much narrower and converge to the exact input soil parameters, especially for M and ν. It seems that the estimation of M and ν was well established first and the values of κ in the 47th generation still have large divergence. Fig. 9 shows the comparison between the calculated wall deflection using the back-estimated optimal parameters with the lowest objective function value in the last generation and the synthetic wall deflection of the benchmark case. As expected there is excellent agreement between the simulations and the synthetic measurements. In general, according to the results of back analyses using the synthetic case, the efficacy and accuracy of the back analysis are satisfactory. It is desirable to incorporate the real excavation case histories to further examine the applicability of the method.

EXAMPLE APPLICATION: TAIPEI NATIONAL ENTERPRISE CENTER

In this study, the excavation of Taipei National Enterprise Center (TNEC) is employed to back analyses soil parameters based on the wall deflection at each excavation stage. The Taipei National Enterprise Center (TNEC) excavation is selected as a comprehensive field monitoring system and large amount of laboratory tests were conducted in this site [12, 54].

Numerical Model of the TNEC Excavation

The TNEC case is located in the Taipei Basin and its typical soil profile of the site is shown in Fig. 10. The ground consists of six alternating silty sand (SM) and silty clay (CL) layers overlying a thick gravel formation. The silty clay layers are mainly low-plasticity and slightly over-consolidated soft to medium clay. The gravel layer is located 46 m below the ground surface. The excavation was conducted using the

top-down construction method in seven stages. The final excavation depth was 19.7 m. A 0.9 m thick and 35 m deep diaphragm wall which was supported by two levels of horizontal struts and five levels of 150 mm thick concrete floor slabs was used as the retaining structure. Fig. 10 also illustrates the sequences of excavation and the horizontal supporting system. Detailed information of TNEC case can be referred to [12, 54].

Fig. 11 shows the finite element mesh used in this analysis. To reduce the computational load, only half of the excavation is modeled according to symmetry. The right boundary is 100 m away from the excavation center and is well beyond the influence zone of excavation, which is normally around four times of the excavation depth. The bottom boundary is set at the surface of the gravel soil layer, i.e., 46 m below the surface. The boundary conditions in the synthetic case were implemented here, which means that the horizontal and rotational freedom was fixed on the left side, the horizontal and vertical freedom was fixed on the bottom and only the horizontal freedom was fixed on the right side.

In the FEM model, the clayey soil layers (CL) and the sandy soil layers (SM) were simulated by Modified Cam-clay (MCC) model and Mohr-Coulomb (MC) model, respectively. In this study, drained condition is assumed and effective stress constitutive models are for both sand and clay soils. Table 3 presents the input parameters for the sandy soil layers. For the sandy soil layers, the effective frictional angle ϕ' is obtained from direct shear tests. According to Ou and Lai [2], the Young's modulus E of sandy soils can be estimated from the following equation:

$$E = 2\beta\rho V_s^2(1+\nu) \tag{7}$$

where ρ is the soil density; V_s is the shear wave velocity and can be estimated using an empirical equation with the SPT N value; β is a reduction factor which considers the difference between small strain and the strain at the normal condition and the β value can be set equal to 0.5 based on experience [52]. The soil cohesion c and the

dilatancy angle ψ were both set as zero for the SM layers. Based on the sensitivity analysis in the previous section, the three soil parameters, i.e., ν, κ and M, are identified as the most important parameters of the MCC model. Therefore, in this case study, total nine soil parameters of the three clay layers are chosen to be estimated in the back analysis. Table 4 lists the upper and lower bounds of these three parameters with the consideration to cover most possible values of MCC model parameters for clayey soils [25, 51, 55]. For the clayey soil layers, the logarithmic compression index, λ, is equal to $C_c/2.303$, where C_c is the compression index. The in situ at rest earth pressure coefficient (K_0) is estimated using the Jacky's equation: $K_0 = 1 - \sin(\phi')$.

The Young's modulus of the diaphragm wall used in the analysis is 12 GPa and the Poisson's ratio is assumed to be 0.2 based on Ou et al. [54]. The average nominal axial stiffness per unit width for the first strut level and the second strut level are 14,980 KN/m/m and 64,363 KN/m/m respectively. As preloading forces were applied to the struts during the installation procedure, the strut forces are taken as 98.1KN/m and 392KN/m for the first and second temporal horizontal struts, respectively. The axial stiffness of the concrete floor slabs is assumed to be 146,512 KN/m/m, which is about 80% of its nominal value, considering the reduction of the concrete stiffness due to large bending moment of the diaphragm wall and the occurrence of cracks in the concrete. Since the wall friction coefficient has a relatively small effect on the wall deflection as shown in the previous sensitivity analysis, the friction coefficient of the wall-soil interface, μ, is assumed to be a constant value of 0.273, which represents the weighted average of μ along the whole length of the diaphragm wall.

Identification of Soil Parameters for Each Excavation Stage

The same control parameters of differential evolution as in the synthetic case are implemented in TNEC case with 90 ($10 \times m$) individual vectors in each generation. The field measured wall deflection at each stage of excavation is used to back analyze the nine soil parameters. When the number of generation reaches 100 or when the

value objective function is less than 1.0%, the back analysis process is terminated. The computation load for this case study is very heavy if we use a normal laptop computer. For each excavation stage, maximum 9,000 simulations (100 generations) have to be calculated in FE analysis program. For back analysis for all the seven stages, the computer time could be months in a normal computer. In this study, the simulations for 90 parameter vectors in one generation are submitted at the same time in a super computer cluster with 500 2.3GHz cores, so the calculation time is dramatically reduced to only a few hours. Fig. 12 shows the boxplots for back estimated parameters, ν, κ and M, of three clayey layers. The x axis of the graph, S1 to S7, denotes the seven stages of the excavation. It can be seen that the ranges for all nine parameters except M of the fifth soil layer, are significantly narrowed. For the first soil layer, the back estimated soil parameters for the seven excavation stages are very close. For the third soil layer which influences the wall deflection, the back estimated parameters vary with the excavation stages and gradually reach steady values at the final stage. The parameters of the fifth soil layer varied significantly with excavation stage and the parameter M has a wide distribution. It is mainly because the fifth layer is below the excavation base and has limited influence on the wall deflection. Therefore, it is hard to determine the parameters for the fifth layer through back analysis using the observed wall deflection.

The estimated wall deflections using the back-analyzed soil parameters with the optimal objective function in each stage are compared with the field observation as shown in Fig. 13. The values of objective function in terms of the relative error of the estimated wall deflection for the seven stages are 9.7%, 16.5%, 12.8%, 5.2%, 2.2%, 1.1% and 1.0%, respectively. It can be seen that the estimated wall deflections are very close to the field measurements especially for the last three stages. For the first three stages, the estimated wall deflection seems not agree well with the field measured values, especially for the first stage. This is because the objective function is the relative error while the measured wall deflections of the first three stages are

563 relatively small. In addition, the wall deflections in the first three stages are
564 significantly affected by the second soil layer, which is a sandy soil layer and the soil
565 properties of the sand soil layers are constant values and are not tuned in the back
566 analysis. The results obtained in this study for stage 5-7 are comparable to the relative
567 errors (2.70%, 1.07%, and 2.84% for stage 5-7, respectively) obtained by NOT
568 algorithm (nonlinear optimization technique with a quasi-Newton method) in Tang
569 and Kung [22]. In Tang and Kung [22], parameters of all six soil layers are back
570 estimated, while in this study only the parameters of clayey layers were back
571 analyzed.

572 **Forward Prediction using Identified Parameters**

573 The practice goal of incorporating the back analysis in excavation is to predict the
574 response of the excavation based on the early stage observations. Therefore, in this
575 example, the input parameters optimized in the early stages of the excavation are used
576 to predict the performance of the excavation at subsequent stages to further examine
577 the capacity of the back analysis methodology and the developed code. The relative
578 errors of prediction for stages 4-7 calculated with the optimized parameters in the
579 previous stages are presented in Fig. 14. The numbers in y-axis represents the stage
580 numbers for prediction. For example, the wall deflection in stage 4 is predicted using
581 the optimized parameters obtained from back analysis of stage 1 to 3 and the relative
582 errors of the prediction are presented in the first row of bullets in y-axis. As shown in
583 the graphs, the wall deflection can be generally satisfactorily predicted using the back
584 analyzed soil parameters at previous stages. A better prediction can be obtained when
585 using the optimized parameters from back analysis of the most recent previous stage
586 than using those from much earlier stages. The reason is that the performance of
587 excavation is not drastically changed between two adjacent stages. The relative errors
588 of prediction by the optimized parameters from stage 1-3 are greater than those
589 obtained using the optimized parameters from stage 4-6. This may due to the large
590 uncertainties of back estimated parameters in the first three stages.

LIMITATIONS

As illustrated in the two examples, the back analysis using the Differential Evolution Genetic Algorithm is a powerful tool for model calibration using field measurement. It can locate the optimized multiple soil parameters within limited computation load and can provide acceptable predictions for subsequent responses of an excavation. However, it is important to note that the process of parameter estimation is carried out in the context of a specified numerical model that includes geometry, boundary conditions and constitutive models for soils. Hence, it is unable to overcome inherent limitations in the selected material constitutive model such as the inability to capture small strain stiffness.

Selecting a proper objective function is very important in inverse analysis and the one implemented in this study gives preference to small values and it may be affected by the number of measurement points. The uncertainty in the field measurements is not considered in this study. Effect of different types of objective functions is out of the scope of this study and will be further investigated in another paper.

In this study, the soils in the excavation are assumed to be drained. As the construction of an excavation usually takes several months, the soil behaviors are more likely partially drained [52]. A coupled hydro-mechanical analysis is more appropriate for such condition. Coupled analysis is out of the scope of this study and will be considered in further research studies.

CONCLUSIONS

The paper demonstrated the potential application of a global optimization method, Differential Evolution (DE) algorithm, in the back-analysis of the deep excavation problems. Wall deflection data are used as observations in an inverse analysis that calibrates the parameters of soil model. The performance of the developed Differential Evolution algorithm code PyDE which is integrated in the commercial software

618 ABAQUS is illustrated using a synthetic case and a real case of excavation. The
619 following conclusions can be made:
620 (1) The distributions of multiple input soil parameters are well identified after the
621 back-analysis using DE optimization algorithm. For the synthetic excavation case, the
622 back-analyzed parameters are basically identical to the input parameters which are
623 used to generate synthetic response of wall deflection.
624 (2) For the TNEC case with totally nine parameters to be back-analyzed, a
625 satisfactory agreement between simulated response using the back estimated
626 parameters and field monitored performance is obtained. The relative errors of wall
627 deflection for the last three stages are 2.2%, 1.1% and 1.0%, respectively. This
628 illustrates good performance of convergence and efficiency for complex and nonlinear
629 deep excavation problem.
630 (3) In addition, with the back estimated soil parameters at given stage, the wall
631 deflection at subsequent stages can be well predicted. The parameters estimated make
632 a better prediction for the most recent previous stage than for much earlier stages,
633 since similar performance can be observed for two adjacent stages.
634

635 ## ACKNOWLEDGEMENTS

636 The work in this paper was substantially supported by grants from the Natural Science
637 Foundation of China (Project No. 41172252). The authors are grateful for the support
638 from Shanghai Rising-Star Program of Science and Technology Commission of
639 Shanghai Municipality (Project No. 12QA1401800).

640

641 **REFERENCES**

642 1. Finno RJ, Harahap IS. Finite element analyses of HDR-4 excavation. *Journal of*
643 *Geotechnical and Geoenvironmental Engineering* (ASCE) 1991; **117**(10):
644 1590–1609.
645 2. Ou CY, Lai CH. Finite-element analysis of deep excavation in layered sandy and
646 clayey soil deposits. *Canadian Geotechnical Journal* 1994; **31**(2): 204–214.
647 3. Hashash YMA, Whittle AJ. Ground movement prediction for deep excavations in
648 soft clay. *Journal of Geotechnical and Geoenvironmental Engineering* (ASCE)
649 1996; **122**(6): 474–486.
650 4. Ng CWW, Yan WM. Three-dimensional modelling of a diaphragm wall
651 construction sequence. *Geotechnique* 1999; **49**(6), 825–834.
652 5. Zdravkovic L, Potts DM, St John HD. Modelling of a 3D excavation in finite
653 element analysis. *Geotechnique* 2005; **55(**7): 497–513.
654 6. Kung GTC, Hsiao ECL, Juang CH. Evaluation of a simplified small-strain soil
655 model for analysis of excavation-induced movements. *Canadian Geotechnical*
656 *Journal* 2007; **44**: 726–736.
657 7. Nikolinakou M, Whittle A, Savidis S, Schran U. Prediction and Interpretation of
658 the Performance of a Deep Excavation in Berlin Sand. *Journal of Geotechnical*
659 *and Geoenvironmental Engineering* (ASCE) 2011; **137**(11): 1047–1061.
660 8. Burland JB. Ninth Laurits Bjerrum Memorial Lecture: 'Small is beautiful' - the
661 stiffness of soils at small strains." *Canadian Geotechnical Journal* 1989; **26**(4):
662 499–516.
663 9. Zhang LM, Li X. Microporosity structure of coarse granular soils. *Journal of*
664 *Geotechnical and Geoenvironmental Engineering* (ASCE) 2010; **136**(10):
665 1425–1436.
666 10. Li JH, Zhang LM. Connectivity of a network of random discontinuities.
667 *Computers and Geotechnics* 2011; **38**(2): 217–226.
668 11. Lim A, Ou CY, Hsieh PG. Evaluation of clay constitutive models for analysis of

669 deep excavation under undrained conditions. *Journal of GeoEngineering* 2010;
670 **5**(1): 9–20.
671 12. Ou CY, Liao JT, Lin HD. Performance of diaphragm wall constructed using
672 top-down method. *Journal of Geotechnical and Geoenvironmental Engineering*
673 (ASCE) 1998; **124**(9): 798–808.
674 13. Tan Y, Wei B. Observed behaviors of a long and deep excavation constructed by
675 cut-and-cover technique in shanghai soft clay. *Journal of Geotechnical and*
676 *Geoenvironmental Engineering* (ASCE) 2012; **138**(1): 69–88.
677 14. Wu S, Ching J, Ou C. Predicting Wall Displacements for Excavations with Cross
678 Walls in Soft Clay. *Journal of Geotechnical and Geoenvironmental Engineering*
679 (ASCE) 2012; DOI: http://dx.doi.org/10.1061/(ASCE)GT.1943-5606.0000826.
680 15. Ledesma A, Gens A, Alonso EE. Estimation of parameters in geotechnical
681 backanalysis - I. Maximum likelihood approach. *Computers and Geotechnics*
682 1996; **18**(1): 1–27.
683 16. Rechea C, Levasseur S, Finno R. Inverse analysis techniques for parameter
684 identification in simulation of excavation support systems. *Computers and*
685 *Geotechnics* 2008; **35**(3): 331–345.
686 17. Finno RJ, Calvello M. Supported excavations: Observational method and inverse
687 modeling. *Journal of Geotechnical and Geoenvironmental Engineering* (ASCE)
688 2005, **131**(7), 826–836.
689 18. Zhang J, Tang WH, Zhang LM. Efficient probabilistic back-analysis of slope
690 stability model parameters. *Journal of Geotechnical and Geoenvironmental*
691 *Engineering* (ASCE) 2010; **136**(1): 99–109.
692 19. Zhang LL, Zhang J, Zhang LM, Tang WH(2010). Back analysis of slope failure
693 with Markov chain Monte Carlo simulation. *Computers and Geotechnics* 2010;
694 **37**(7–8): 905–912.
695 20. Zhang LL, Zuo ZB, Ye GL, Jeng DS and Wang JH. Probabilistic parameter
696 estimation and predictive uncertainty based on field measurements for

unsaturated soil slope. *Computers and Geotechnics* 2013; **48**(1): 72–81.

21. Juang CH, Luo Z, Atamturktur S, Huang H. Bayesian Updating of Soil Parameters for Braced Excavations Using Field Observations. *Journal of Geotechnical and Geoenvironmental Engineering (ASCE)* 2013; **139**(3): 395–406.

22. Tang YG, Kung GTC. Application of nonlinear optimization technique to back analyses of deep excavation. *Computers and Geotechnics* 2009; **36**(1–2): 276–290.

23. Hashash YMA, Marulanda C, Ghaboussi J, Jung S. Novel approach to integration of numerical modeling and field observations for deep excavations. *Journal of Geotechnical and Geoenvironmental Engineering* (ASCE) 2006; **132**(8): 1019–1031.

24. Levasseur S, Malécot Y, Boulon M, Flavigny E. Soil parameter identification using a genetic algorithm. *International Journal for Numerical and Analytical Methods in Geomechanics* 2008; **32**(2): 189–213.

25. Zentar R, Hicher PY, Moulin G. Identification of soil parameters by inverse analysis. *Computers and Geotechnics* 2001; **28**(2): 129–144.

26. Zhang Y, Gallipoli D, Augarde CE. Simulation-based calibration of geotechnical parameters using parallel hybrid moving boundary particle swarm optimization. *Computers and Geotechnics* 2009; 36(4): 604–615.

27. Obrzud RF, Truty A, Vulliet L. Numerical modeling and neural networks to identify model parameters from piezocone tests: II. Multi-parameter identification from piezocone data. *International Journal for Numerical and Analytical Methods in Geomechanics* 2012; **36**(6): 743–779.

28. Levasseur S, Malecot Y, Boulon M, Flavigny E. Statistical inverse analysis based on genetic algorithm and principal component analysis: Method and developments using synthetic data. *International Journal for Numerical and Analytical Methods in Geomechanics* 2009; **33**: 1485–1511.

29. Levasseur S, Malecot Y, Boulon M, Flavigny E. Statistical inverse analysis based

on genetic algorithm and principal component analysis: Applications to excavation problems and pressuremeter tests. *International Journal for Numerical and Analytical Methods in Geomechanics* 2010; **34**: 471–491.

30. Simpson AR, Priest SD. Application of genetic algorithms to optimization problems in geotechnics. *Computers and Geotechnics* 1993; **15**(1): 1–19.
31. Kemeny J, Post R. Estimating three-dimensional rock discontinuity orientation from digital images of fracture traces. *Computers and Geosciencs* 2003; **29**(1): 65–77
32. Guan Z, Jiang Y, Tanabashi Y. Rheological parameter estimation for the prediction of long-term deformations in conventional tunnelling. *Tunnelling and Underground Space Technology* 2009; **24**(3): 250–259
33. Papon A, Riou Y, Dano C, Hicher P-Y. Single- and multi-objective genetic algorithm optimization for identifying soil parameters. *International Journal for Numerical and Analytical Methods in Geomechanics* 2012; **36**: 597–618.
34. Zolfaghari AR, Heath AC, McCombie PF. Simple genetic algorithm search for critical non-circular failure surface in slope stability analysis. *Computers and Geotechnics* 2005; **32**: 139–152
35. Xue J-F, Gavin K. Simultaneous determination of critical slip surface and reliability index for slopes. *Journal of Geotechnical and Geoenvironmental Engineering (ASCE)* 2007; **133**(7): 878–886
36. Chan C, Zhang L, Ng J. Optimization of pile groups using hybrid genetic algorithms. *Journal of Geotechnical and Geoenvironmental Engineering (ASCE)* 2009; **35**(4): 497–505.
37. Cui LJ, Sheng DC. Genetic algorithms in probabilistic finite element analysis of geotechnical problems. *Computers and Geotechnics* 2005; **32**: 555–563
38. Hashash YMA, Levasseur S, Osouli A, Finno R, Malecot Y. Comparison of two inverse analysis techniques for learning deep excavation response. *Computers and Geotechnics* 2010; **37**(3): 323–333.

753 39. Holland JH. *Adaptation in Natural and Artificial Systems: An Introductory*
754 *Analysis with Applications to Biology, Control and Artificial Intelligence*. MIT
755 Press: Cambridge MA, 1992.
756 40. Babu BV, Sastry KKN. Estimation of heat transfer parameters in a trickle-bed
757 reactor using differential evolution and orthogonal collocation. *Computers &*
758 *Chemical Engineering* 1999; **23**(3): 327-339
759 41. Storn R, Price K. Differential evolution - A simple and efficient heuristic for
760 global optimization over continuous spaces. *Journal of global optimization* 1997;
761 **11**(4): 341–359.
762 42. Price KV, Storn RM, Lampinen JA. *Differential Evolution – A Practical Approach*
763 *to Global Optimization*. Springer: Germany, 2005.
764 43. Chakraborty UK. *Advances in Differential Evolution*. Springer: Berlin, Germany,
765 2008
766 44. Das S, Suganthan PN. Differential Evolution: a survey of the state-of-the-art.
767 *IEEE Transactions on Evolutionary Computation* 2011; 15(1):4-31. doi:
768 10.1109/TEVC.2010.2059031
769 45. Amorim EP, Xavier CR, Campos RS, Rodrigo W. Comparison between genetic
770 algorithms and differential evolution for solving the history matching problem. In
771 *Computational Science and Its Applications, Proccedings of ICCSA 2012*.
772 Murgante B et al. (eds.) Lecture Notes in Computer Science Volume 7333,
773 Salvador de Bahia, Brazil, June 18-21. Springer: Verlag Berlin Heidelberg 2012;
774 635-648.
775 46. Vardakos S, Gutierrez M, Xia C. Parameter identification in numerical modeling
776 of tunneling using the Differential Evolution Genetic Algorithm (DEGA).
777 *Tunnelling and underground space technology* 2012; **28**(1): 109–123.
778 47. Xing J, Jiang A, Wen Z, Qiu J. A nonlinear optimization technique of tunnel
779 construction based on DE and LSSVM. *Mathematical Problems in Engineering*
780 2013; Article ID 980154, 11 pages. doi:10.1155/2013/980154

48. Lampinen J. A constraint handling approach for the Differential Evolution Algorithm. In *Proceedings of the 2002 IEEE Congress on Evolutionary Computation*, Honolulu Hawaii: 1468–1473.
49. Fourie AB, Potts DM. Comparison of finite element and limiting equilibrium analyses for an embedded cantilever retaining wall. *Geotechnique* 1989; **39**(2): 175–188.
50. Bica AVD, Clayton CRI. An experimental study of the behaviour of embedded lengths of cantilever walls. *Geotechnique* 1998; **48**(6): 731–745.
51. Navarro V, Candel M, Barenca A, Yustres A, Garcia B. Optimisation procedure for choosing Cam clay parameters. *Computers and Geotechnics* 2007; **34**(6): 524–531.
52. Ou CY. Deep Excavation: Theory and Practice. *Taylor & Francis*: Netherlands, 2006.
53. Frey HC, Patil SR. Identification and review of sensitivity analysis methods. *Risk Analysis* 2002; **22**(3): 553-578.
54. Ou CY, Shiau BY, Wang IW. Three-dimensional deformation behavior of the Taipei National Enterprise Center (TNEC) excavation case history. *Canadian Geotechnical Journal* 2000; **37**(2): 438–448.
55. Yin ZY, Hicher PY. Identifying parameters controlling soil delayed behaviour from laboratory and in situ pressuremeter testing. *International Journal for Numerical and Analytical Methods in Geomechanics* 2008; **32**(12): 1515–1535.

LIST OF TABLES

LIST OF FIGURES

836 Table 1. Soil parameters used in the parametric study of the synthetic case

Soil Parameters	ν	κ	λ	M	μ
	0.1	0.007	0.07	0.8	0.1
Benchmark value	0.2	0.014	0.14	1.2	0.2
	0.3	0.021	0.21	1.6	0.3

837

838

839 Table 2. Back-analyzed soil parameters for the synthetic case

Parameter	True value	Min	Max	Optimal value
ν	0.2	0.1	0.3	0.2026
κ	0.014	0.007	0.021	0.0137
M	1.2	0.8	1.6	1.1997

840

841

842

843

844

845

846

847

848

849

850

851

852

853

854

855

856 Table 3. Soil properties of SM soil layers in the TNEC case

Soil Layer	Depth (m)	γ (kN/m3)	c (kPa)	ϕ' (°)	Dilatancy angle ψ (°)	E (kPa)	K_0	ν
2	5.6-8	18.9	0	30	0	68351	0.49	0.3
4	33-35	19.6	0	33	0	265473	0.49	0.3
6	37.5-46	19.6	0	35	0	300247	0.47	0.3

857

858

859 Table 4. Soil parameters of CL soil layers in the TNEC case

Soil Layer	Depth (m)	γ (kN/m3)	λ	K_0	e_0	κ	ν	M
1	0-5.6	18.3	0.152	1.0	1.067	[0.01，0.05]	[0.1，0.35]	[0.8, 1.6]
3	8-33	18.9	0.152	0.51	0.820	[0. 01，0.05]	[0.1，0.35]	[0.8, 1.6]
5	35-37.5	18.2	0.152	0.52	0.824	[0. 01，0.05]	[0.1，0.35]	[0.8, 1.6]

860

861

862

863

864

865

866

867

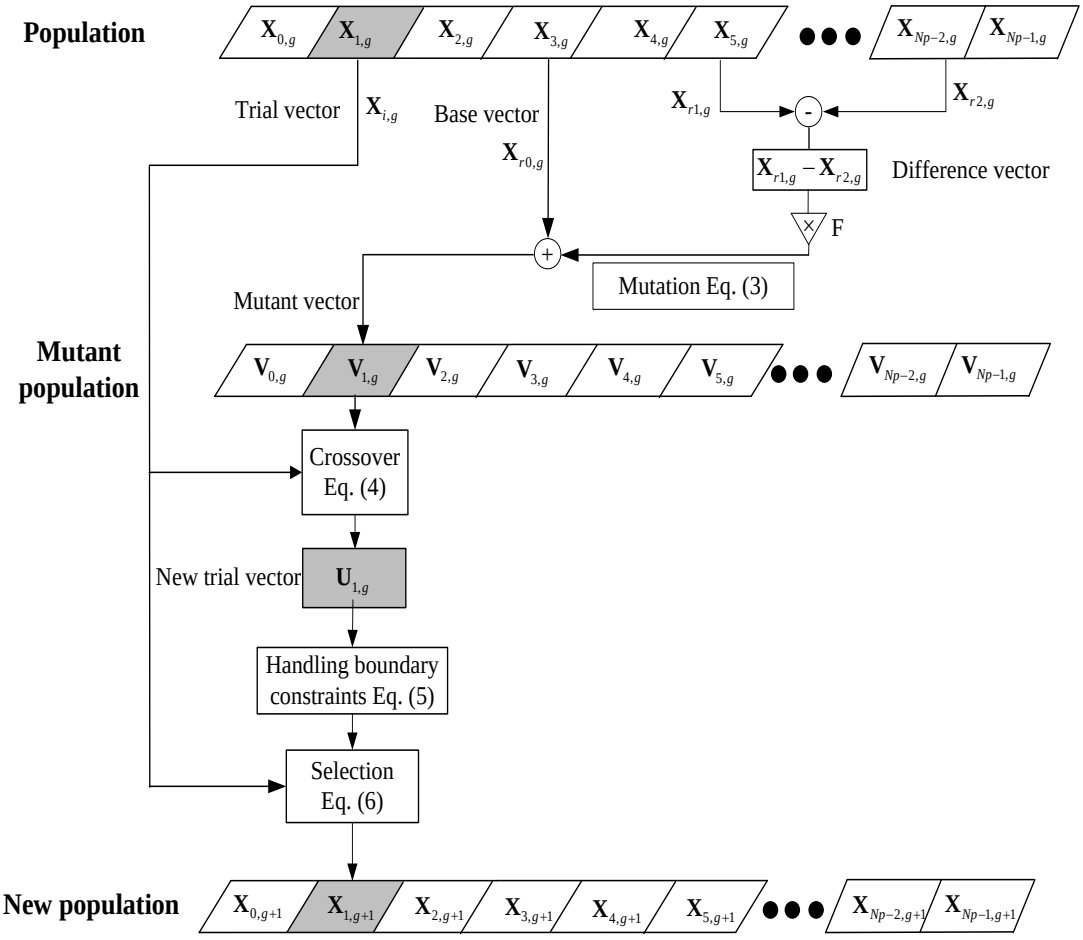

Figure 1. Flow chart of Differential Evolution

(a) (b)

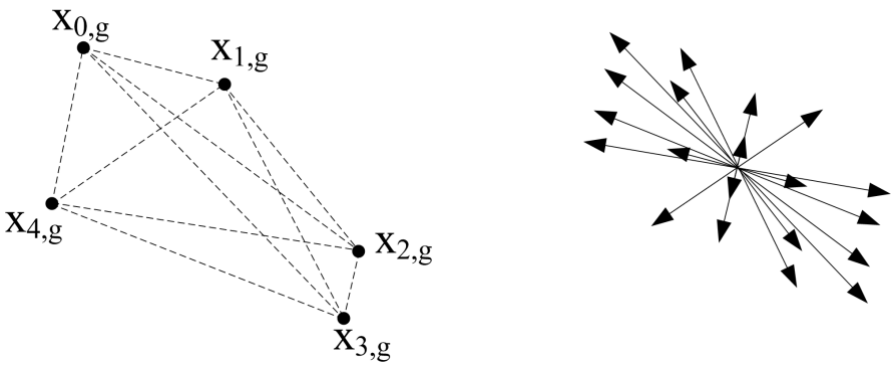

Figure 2. Illustration of difference vectors in a population of 5 vectors: (a) five vectors; (b) non-zero difference vectors scaled by half (F = 0.5), and transported to a common origin (adopted from Price et al. [42])

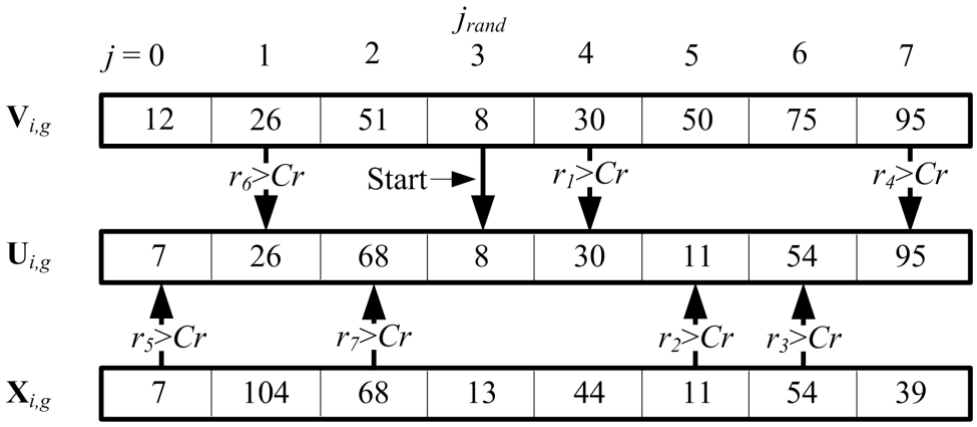

Figure 3. Schematic plot of binary n-point crossover in DE (adopted from Price et al. [42])

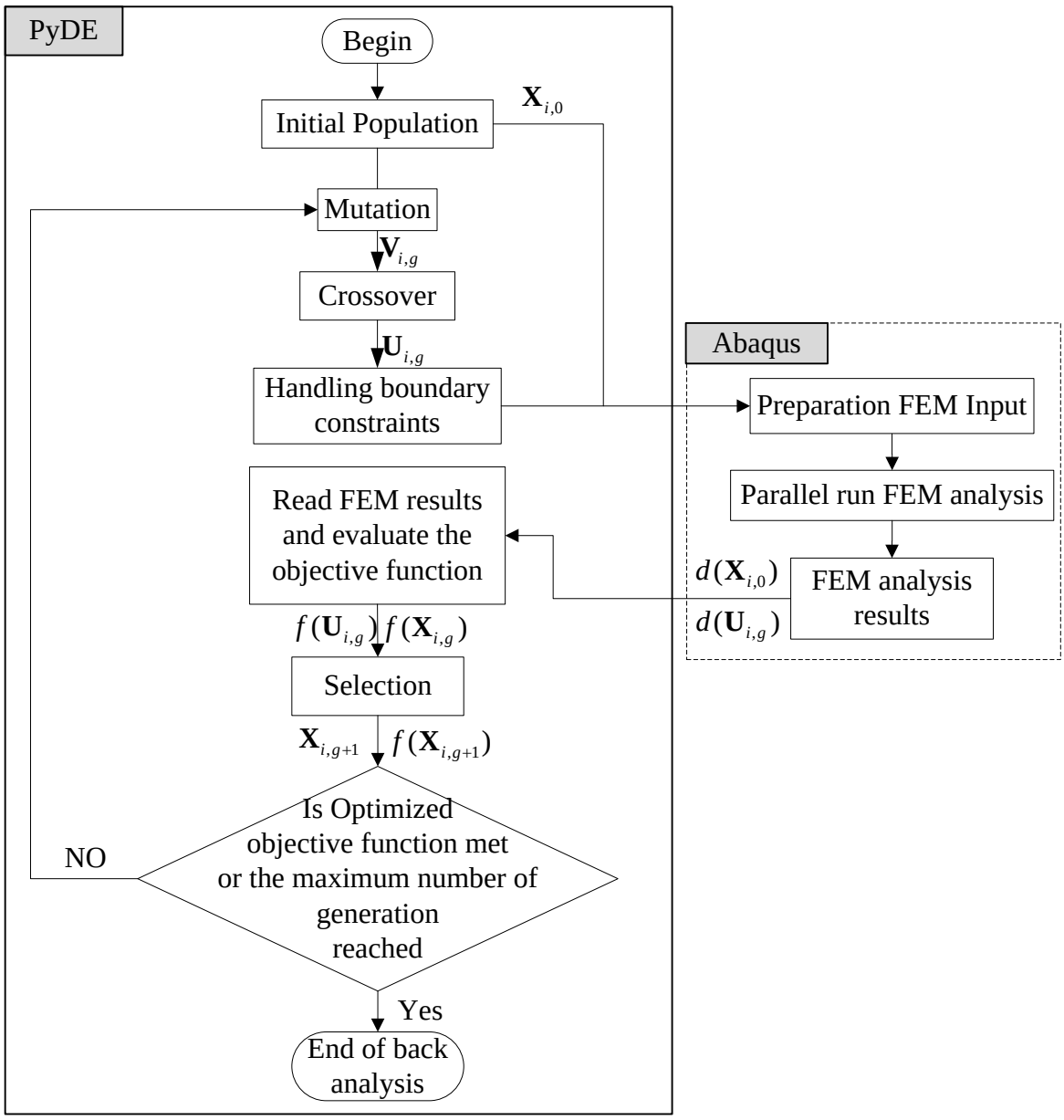

Figure 4. Back analysis with interaction between PyDE code and ABAQUS

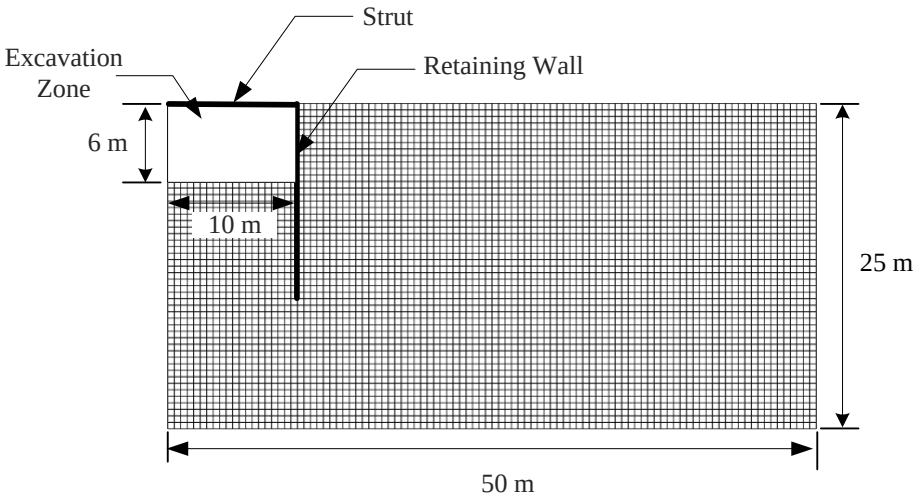

922

923 Figure 5. Geometry and finite element mesh of the synthetic excavation case

924

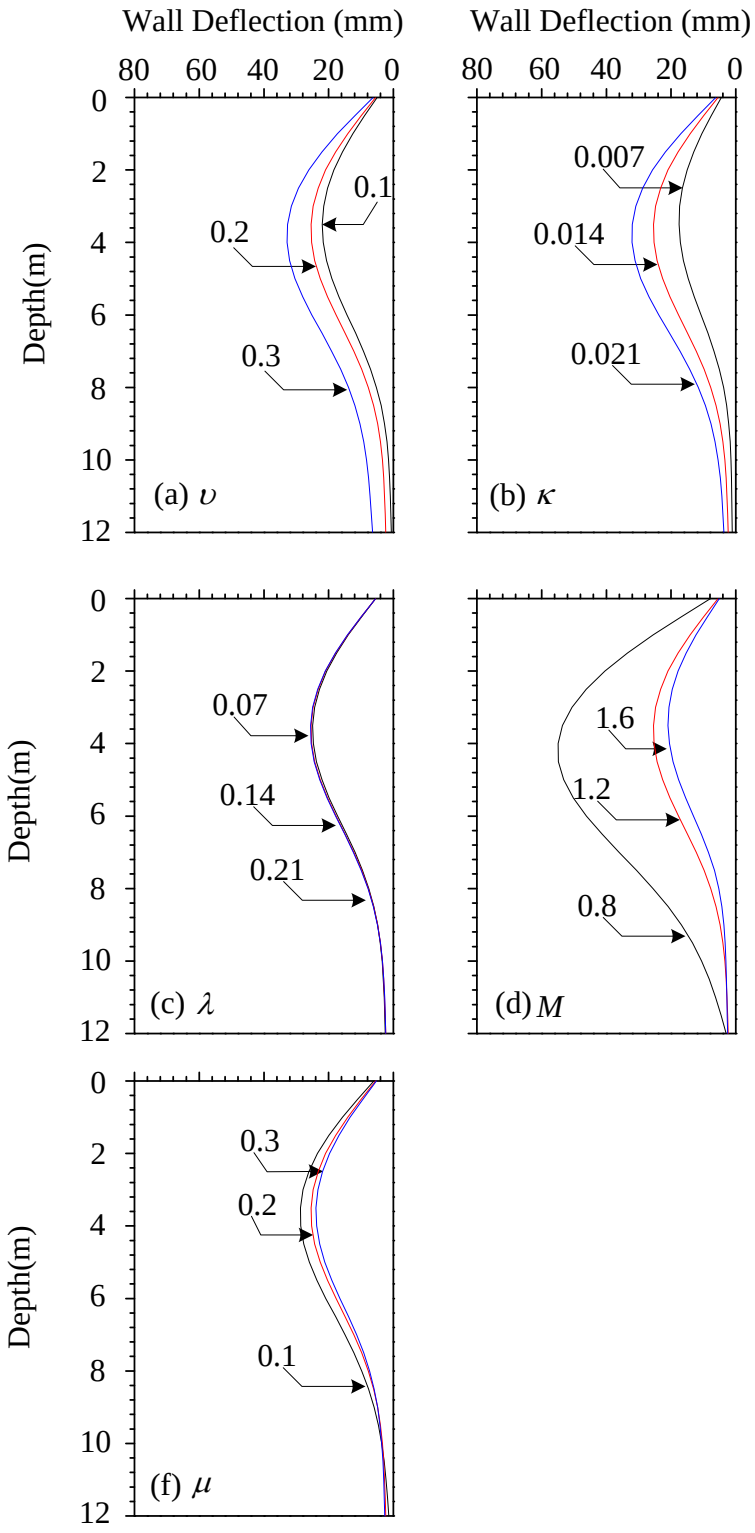

925

926 Figure 6. Effects of soil parameters on wall deflection of the synthetic excavation.

927

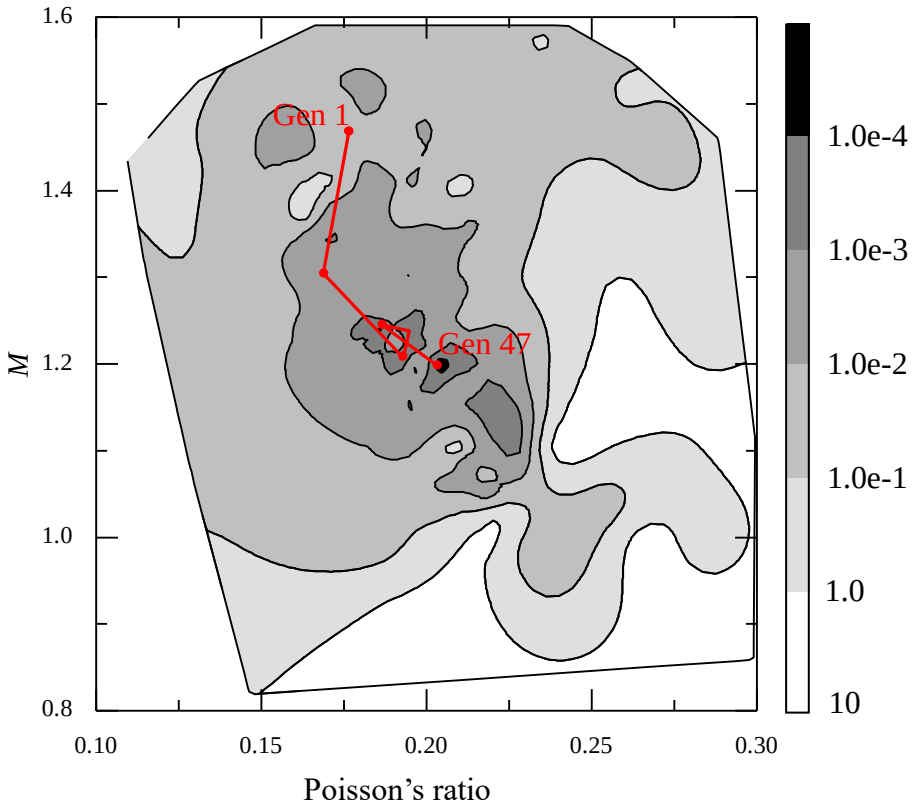

928

929 Figure 7. Contours of the objective function and iteration paths for ν and M

930

931

932

933

934

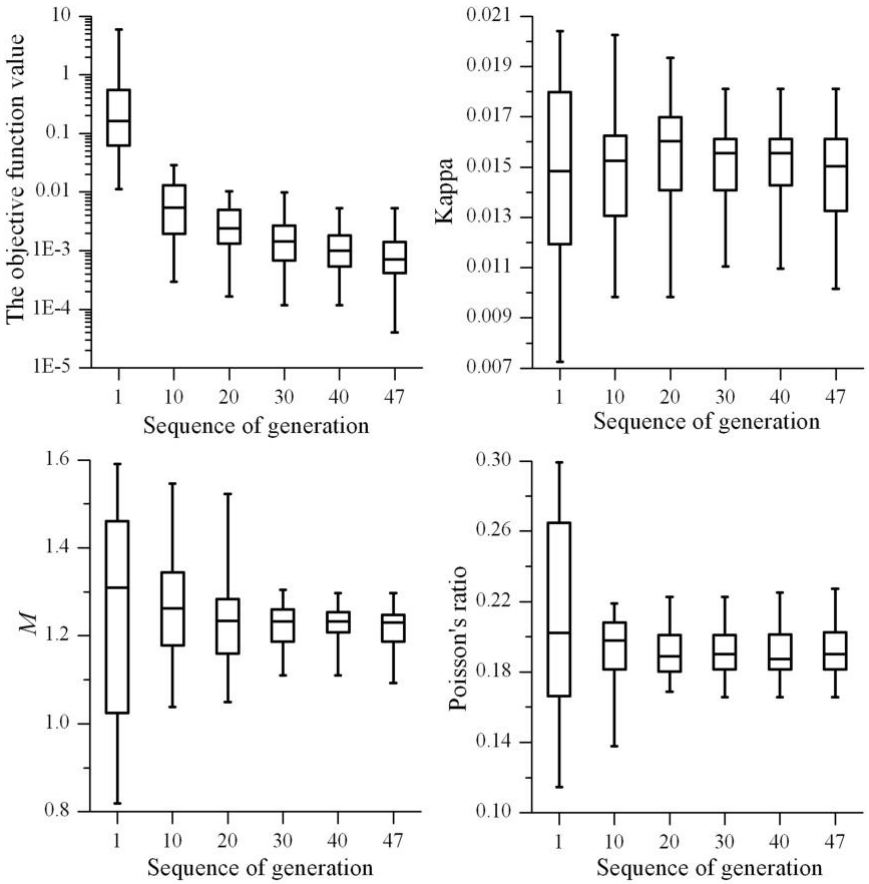

Figure 8. Evolution process of objective function values and soil parameters

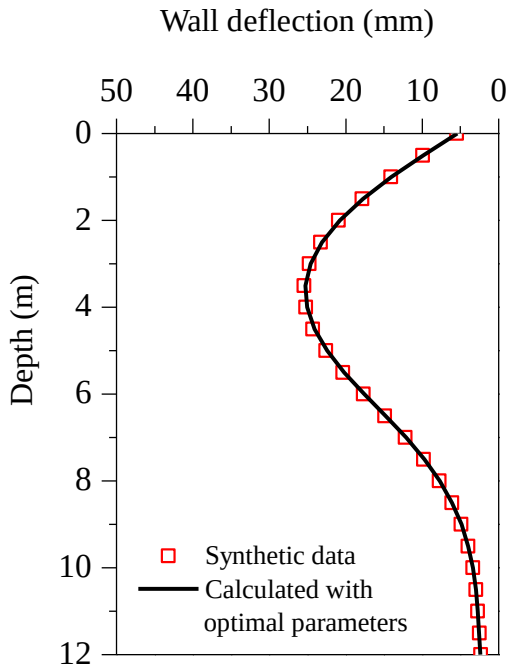

Figure 9. Comparison between the synthetic measurement and the calculated wall deflection based on optimal soil parameters for the synthetic excavation case

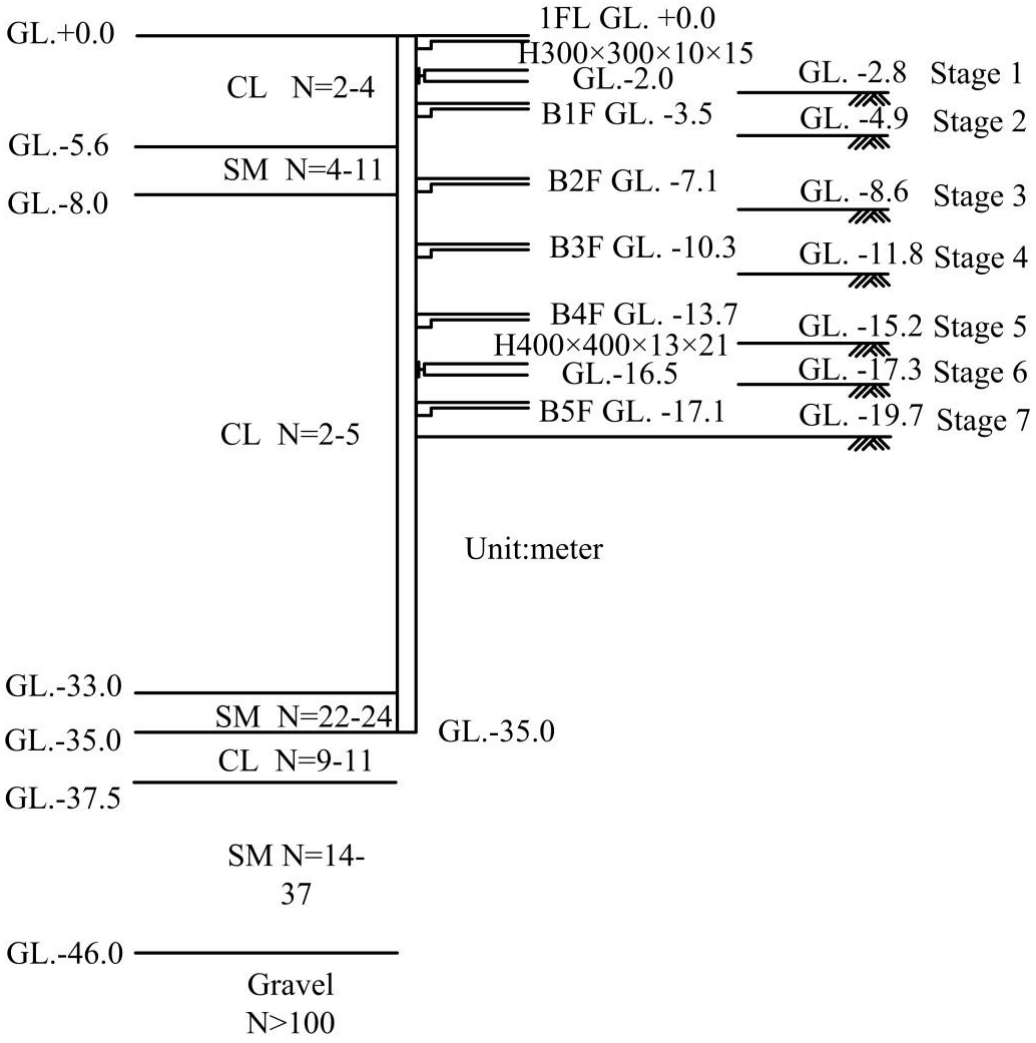

955

956 Figure 10. Construction sequence of excavation and geology profile of TNEC

957 excavation project

958

959

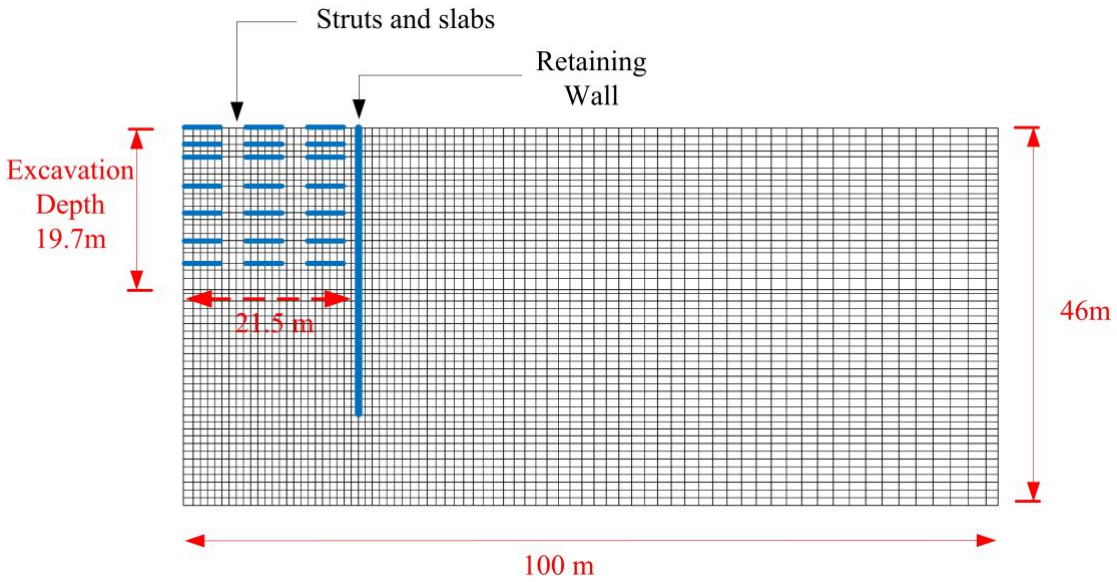

Figure 11. Finite element mesh of the TNEC case

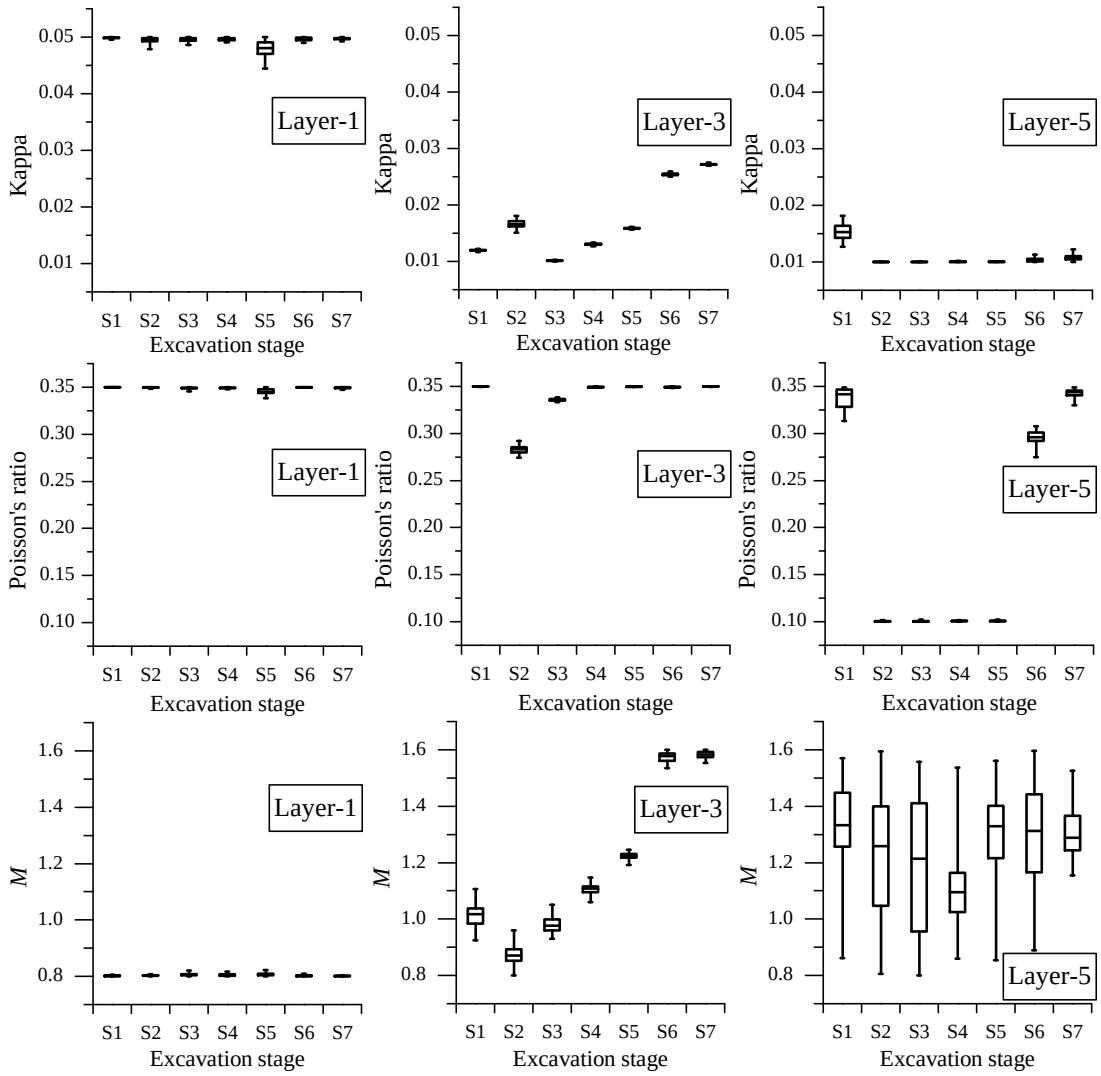

Figure 12. Boxplots of the back-analyzed parameters of TNEC site

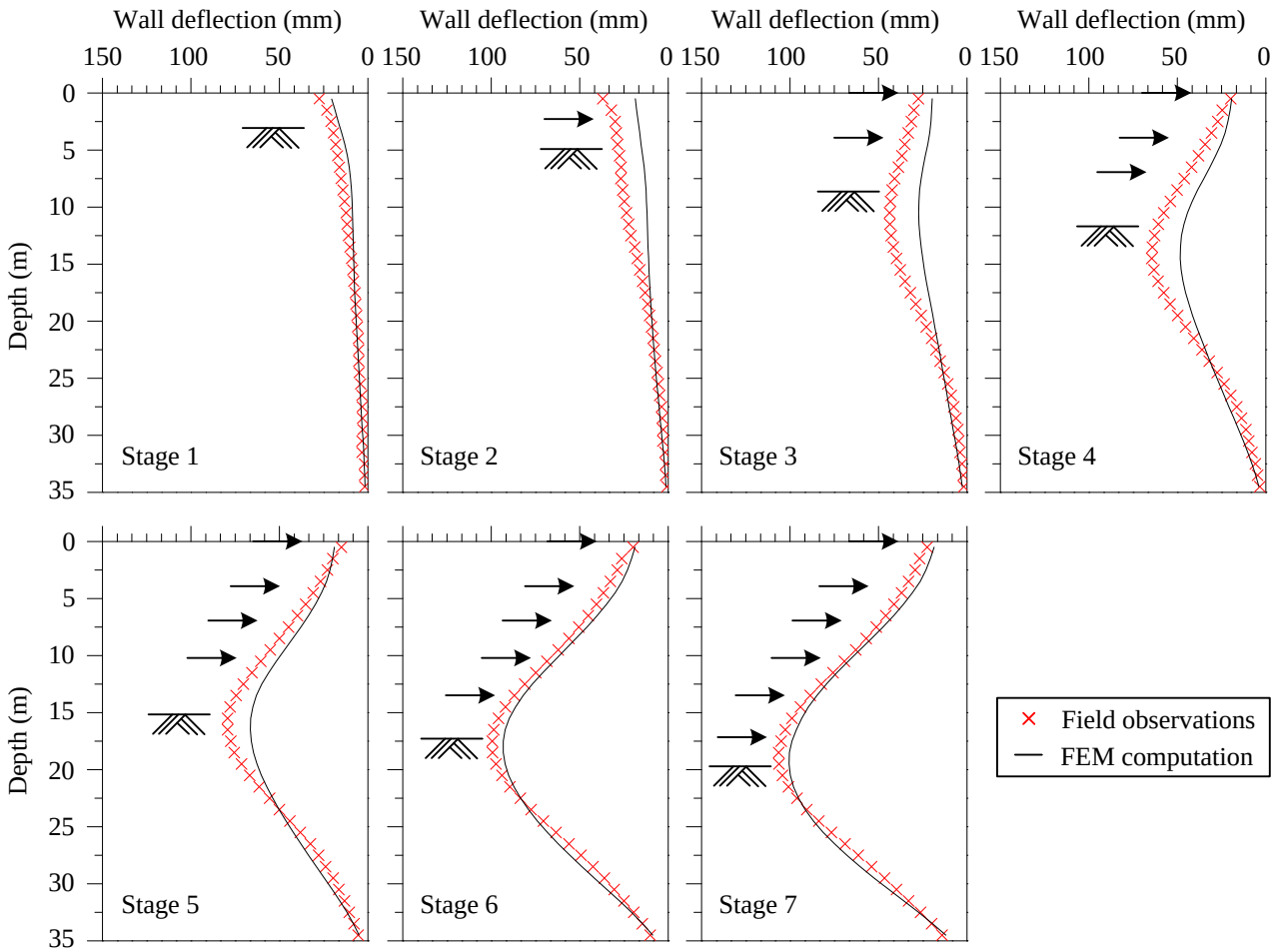

Figure 13. Comparison of observed and calculated wall deflections at various excavation stages

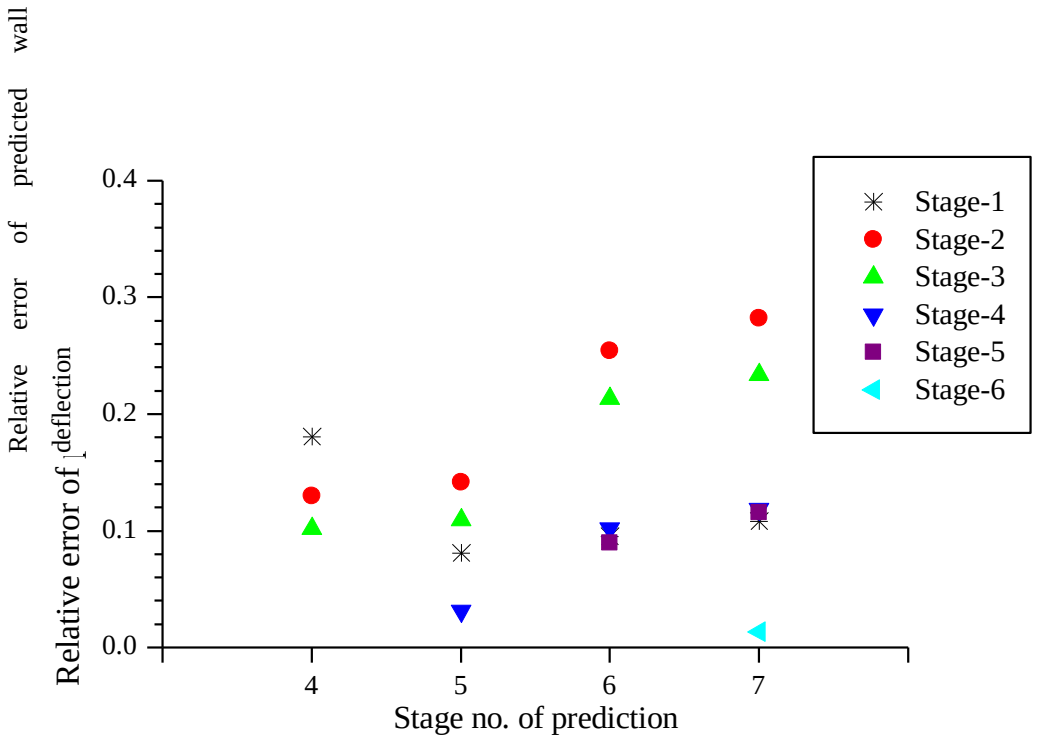

Figure 14. Relative error of prediction at each stage with optimized parameters obtained from back analysis of previous stages